JOURNAL OF MATERIALS SCIENCE 17 (1982) 1108–1116

Fatigue analysis of brittle materials using indentation flaws

Part 2 *Case study on a glass-ceramic*

R. R. COOK, B. R. LAWN*, G. R. ANSTIS†
Department of Applied Physics, School of Physics, University of New South Wales, Kensington, NSW 2033, Australia

The results of an experimental dynamic fatigue study on glass-ceramic specimens containing indentation flaws are analysed in terms of the theory developed in Part 1. A Vickers indenter is used to introduce the flaws, and a conventional four-point bend apparatus to break the specimens. Base-line data for testing the essential theoretical predictions and for evaluating key material/environment parameters are obtained from "polished" surfaces, i.e. surfaces prepared to a sufficient finish to ensure removal of any pre-existing spurious stresses. The fatigue tests are carried out in water. Inert strength tests in dry nitrogen are used to "calibrate" appropriate equilibrium fracture parameters, with "dummy" indentations on selected control specimens providing a convenient measure of the critical crack dimensions at failure. Regression analysis of the dynamic fatigue data yields values for "apparent" kinetic parameters, which are converted to "true" kinetic parameters via the transformation equations of Part I. Regeneration of the fatigue function from the theory using the parameters thus determined gives a curve which passes closely through the experimental data points, thereby providing a self-consistent check of the formalism. The implications of the results in relation to the use of macroscopic fracture parameters in the prediction of strength properties for materials with small-scale flaws is an important adjunct to this work. Finally, a recommended procedure for the general testing of dynamic fatigue properties of ceramics using indentation flaws is described.

1. Introduction

In Part 1 of this study [1] we outlined the theoretical framework for evaluating fatigue parameters from tests on as-indented strength specimens. Emphasis was placed on accommodating a residual contact component explicitly into a general fracture mechanics formulation, such as to ensure optimal simplicity and economy in the experimental test programme. Our aim in this paper is to demonstrate, by way of a case study, the practical application of the method.

Accordingly, results are presented here for dynamic fatigue tests on a magnesium aluminosilicate glass-ceramic (Pyroceram C9606, manufactured by Corning Co.) in water. This choice of a "typical ceramic" derives from three considerations: firstly, independent investigations of the fracture properties have been made by other workers; secondly, it is known (from these independent investigations) that the susceptibility to fatigue (as measured inversely by the crack velocity exponent n) is not high, so the sensitivity of the method should be clearly illustrated; third, the material has a reasonably fine microstructure, which is conducive to the production of "well-behaved" radial-crack patterns. A routine two-

*Present address: Fracture and Deformation Division, National Bureau of Standards, Washington, D.C. 20234, USA.
†Present address: Department of Metallurgy and Science of Materials, University of Oxford, Oxford, UK.

0022–2461/82/041108–09$03.58/0

step procedure, indentation by a Vickers diamond pyramid followed by constant-rate flexure to failure, is used to obtain the basic strength data. Requisite values of the critical crack dimensions are obtained by a contrived experiment whereby control specimens containing "dummy" indentations are subjected to post-failure microscopic examination. The theory developed in Part 1 is then used to evaluate the pertinent fracture parameters for the material.

In the course of the analysis due emphasis will be placed on the key role of the residual contact stresses in the fracture mechanics to failure. In addition, attention will be paid to some of the "secondary" effects dealt with in Part 1, e.g. those relating to the surface stress state *prior* to indentation and a multi-region crack velocity function, which are found to have an important bearing on the fatigue response.

2. Test procedure

2.1. Preparation and indentation of glass-ceramic specimens for strength testing

Pyroceram C9606 is a magnesium aluminosilicate glass-ceramic, with cordierite ($2MgO \cdot 2Al_2O_3 \cdot 5SiO_2$) the main crystalline phase. Some minor crystalline phases are also present, among them titania (TiO_2) which is included as a nucleating agent, and $\approx 5\%$ glassy phases. The material has a microstructure in the size range of 1 to 10 μm, but can contain pores of a somewhat larger dimension. More detailed descriptions of the microstructure in relation to strength properties are to be found elsewhere [2, 3].

Specimens suitable for bend testing were supplied to us by B. J. Pletka and S. M. Wiederhorn* in the form of bars 32 mm by 6 mm by 4 mm. These bars were cut from the same billet of material used by Pletka and Wiederhorn in their comparative study of the macroscopic crack growth and fatigue properties of Pyroceram [3, 4]. The surfaces of the bars had all been machined with a 400-grit diamond wheel. Approximately one half of the specimens were given a further surface finish on their prospective tensile faces, using a slurry of 1000-grit SiC to remove a layer > 100 μm; this was done in accordance with a preliminary investigation into the effects of surface state on strength [5], where it was demonstrated that a finish of this kind is effective in removing significant residual stresses due to the relatively severe machining-damage treatment. Of these "polished" specimens, a few were smoothed to a final mirror surface finish with 1 μm diamond paste, to provide optimal reflectivity for ensuing crack observation.

Each bar was then indented with a Vickers diamond pyramid at the centre of its prospective tensile face at a standardized tensile load, $P = 20$ N. This load was selected on the basis of crack-size considerations: on the one hand, the crack should be sufficiently large in comparison with the microstructure and with the scale of the central deformation zone that it may be considered to be "well-developed"; on the other, the crack should always remain small relative to the specimen dimensions. The Vickers pyramid was oriented to produce radial crack traces parallel to the specimen edges. All indentations were made in air, at a fixed load duration of 10 sec. Those specimens prepared with mirror-smooth surfaces were given a special indentation treatment: additional indentations were made along the longitudinal centre-line in the tensile face, giving a total of three within the inner-span region and one in the outer overhang region of the test bar, with each spaced at least 1.5 mm from its neighbours and from the specimen supports (see below) to avoid interaction effects. All indented specimens were allowed to sit for approximately 1 h, in air, before strength testing.

The specimens thus prepared were then broken in four-point flexure, with an inner span of 7.5 mm and an outer span of 24.0 mm. A cross-head testing machine was used to deliver the bending load, which was monitored by two load cells: a conventional strain-gauge instrumented load cell was used for "slow" tests, corresponding to failure times > 1 to 10 sec; for "fast" tests, a piezoelectric cell with a frequency response of 60 kHz, was switched in. Simple beam theory was used to evaluate the stress in the tensile surface. Both cells gave a linear stress–time response at constant cross-head speed; a working range of stress rates of $\dot{\sigma}_a \approx 2.5 \times 10^{-3}$ to 2.5×10^{3} MPa sec^{-1} was available to us with this composite system. The test environment during flexure to failure was controlled in accordance with the special requirements of the strength property under examination, i.e. inert or fatigue strength, as described in the subsections below. All broken test-pieces were examined routinely by optical microscopy to

*Fracture and Deformation Division, National Bureau of Standards, Washington, D.C. 20234, USA

TABLE I Strengths of indented bars

Number of bars	Finish	Environment	Strength (MPa)
14	1000-grit SiC	Air	145 ± 7†
11	1 μm diamond	Dry argon*	147 ± 5

*The bars were placed inside plastic envelopes to confine the gas flow.
†The errors represented standard deviations.

confirm that failure had indeed initiated from the indentation site.

2.2. Inert strength parameters

In the theoretical analysis in Part 1 it was demonstrated that the parameters σ_m and c_m, representing the stress and dimension at the unstable equilibrium configuration for radial cracks driven by applied tensile loading in combination with residual-contact forces, afford a most convenient base for data reduction. This configuration obtains at failure under "inert" environmental conditions, i.e. such that kinetic crack growth effects of the type embodied in the crack–velocity expression Equation 4 of [1] are entirely absent. Accordingly, strength tests were run on the polished, as-indented bars at the fastest available stress rate (2.5 GPa sec^{-1}), the results are shown in Table I. Since these results show no measurable dependence on the environment we may assume (subject to confirmation of the precursor-crack-growth proviso, below) that they correspond closely to true inert strengths, i.e. $\sigma_m = \sigma_i = 146 \pm 6$ MPa (25 combined tests)*. (In this context, it may be noted that similar tests on as-indented soda-lime glass at a stress rate some three orders of magnitude lower than that used here produced indistinguishable strength results in dry nitrogen and vaccum environments [6].) The present tests also indicate that the surface finish, if sufficiently smooth, is not a critical factor; moreover, recalling that the diamond-finished surfaces contained three indentations within the tensile span, it is seen that (at least for the Pyroceram specimens used in our tests) the inert strength is not sensitive to the "multiplicity" of radial cracks.

For the determination of the crack-size parameter, c_m, a post-failure examination was made of the surviving indentations on the diamond-finished surfaces. The frequency of failure was found to be approximately the same for the central as for each of the two flanking indentations within the inner span, as would be expected for non-interacting crack systems within a uniform tensile field. Thus for any given specimen it can be argued that the two surviving indentations from within this inner tensile region must themselves have been on the verge of instability, thus providing us with intact, dummy crack systems for evaluating critical crack dimensions. In this interpretation, those arms of the radial crack systems aligned *perpendicular* to the tensile direction should give a direct measure of c_m; those arms *parallel* to the tension should similarly give a measure of c_0', the crack size prior to strength testing. Fig. 1 is a representative example of the fracture asymmetry observed in a typical dummy system. Actual crack measurements were made by optical microscopy. Owing to the poor crack visibility in the Pyroceram surfaces special care had to be taken to optimize optical conditions, e.g. by flash coating the specimens with gold and using interference contrast at high power (× 700). The values obtained in this way were $c_m = 98 \pm 15$ μm and $c_0' = 69 \pm 13$ μm (22 indentations). By way of reinforcement of the latter determination, measurements were also made of the crack dimensions for those indentations placed in the stress-free, overhang regions of the bend specimens; these measurements, averaged over the four arms of the radial crack system at each indentation, gave $c_0' = 63 \pm 7$ μm (11 indentations). The results confirm that the above-mentioned precursor-crack-growth proviso, $c_0' < c_m$, is satisfied in this material.

Inert strength tests were also run on bars with original machined surfaces, both with and without indentations. For bars with indentations, we obtained $\sigma_i = 212 \pm 12$ MPa (14 bars). This value is some 45% greater than that obtained for polished surfaces with ostensibly identical indentations, reflecting the substantial level of residual compressive stress that can be introduced by heavy machining damage [5]. For machined bars without indentations, the tests gave $\sigma_i = 273 \pm 9$ MPa (10 bars). This result demonstrates that the indentation flaws, while sufficiently large to constitute dominant failure centres in all out tests, are only slightly more severe than the machining flaws.

2.3. Dynamic fatigue tests

For the dynamic fatigue tests proper, the indentation site on each bar was covered with a drop of

*All errors in this paper are standard deviations about the mean, unless specified otherwise.

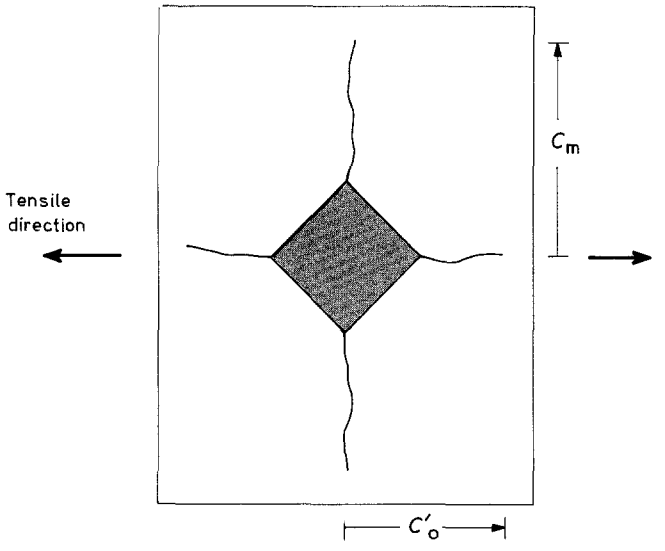

Figure 1 Representation of the radial crack pattern at a dummy indentation in Pyroceram glass-ceramic.

distilled water immediately prior to mounting the bar onto the bending fixture. A glass cover slip was placed over the freshly applied drop to inhibit evaporation during subsequent testing; adhesive tape wound around the covered indentation helped to maintain the specimen intact after failure. For the 1000-grit-polished, as-indented surfaces, an average of 10 bars were broken at each predetermined stress rate. The results are plotted in the conventional manner for dynamic fatigue data, i.e. as log σ against log $\dot{\sigma}_a$, in Fig. 2. This plot becomes our basis for analysing the intrinsic kinetic fracture response of Pyroceram glass ceramic in water environment, in terms of the theory presented in Part 1 (see Section 3, below). It is immediately evident from the data points that the material is susceptible to fatigue, even at the fastest stress rate (which corresponds to a test duration of approximately 50 msec), with a near-linear relation between the logarithmic co-ordinates over the range of stress rates covered.

Comparative test runs were made for the machined, as-indented surfaces to investigate the effect of a pre-indentation surface stress state on fatigue properties. The results of these tests are plotted in Fig. 3, together with the data from Fig. 2 for the polished, similarly-indented surfaces, and from the study of Pletka and Wiederhorn [4] for machined surfaces without indentations. Notwithstanding a greater scatter in individual data points, the machined surfaces show fatigue characteristics distinctly different from those of

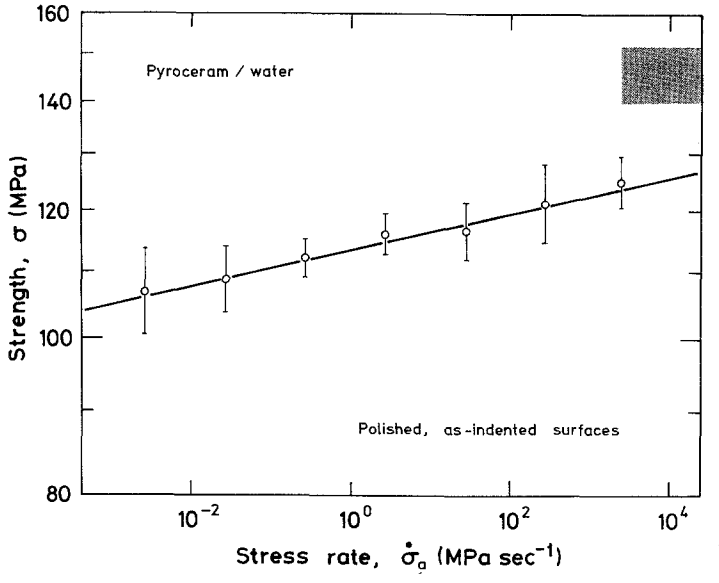

Figure 2 Dynamic fatigue response of Pyroceram glass-ceramic in water, for polished surfaces indented at $P = 20$ N. The shaded band indicates the inert strength level. The degree of fit between the theoretically generated solid curve (using calibrated fracture parameters from inert and fatigue strengths) and the data points may be taken as a measure of the validity of the residual-stress basis of the indentation analysis.

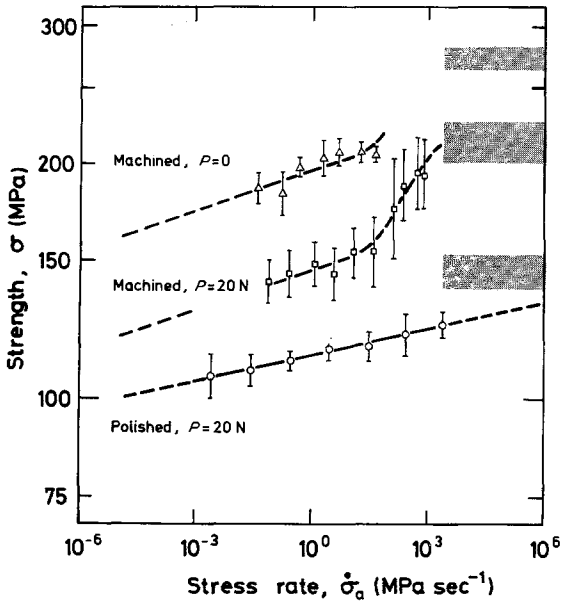

Figure 3 Dynamic fatigue response of Pyroceram glass-ceramic in water, for various surface preparations: polished, as-indented (reproduced from Fig. 2); machined, as-indented; machined surfaces without indentations (reproduced from the study by Pletka and Weiderhorn, [4]). The shaded bands are appropriate inert strength levels. The upper two curves in this plot are approximate fits through the data.

the polished surfaces, most noticeably in the departure from linearity at high stress rates for the as-indented surfaces and in the slopes of the curves in the "linear" region.

3. Analysis of dynamic fatigue data

Let us now consider the results of the previous Section in terms of the theory outlined in Part 1 [1]. The data in Fig. 2 for polished, as-indented surfaces are taken as our reference base. The apparent linearity in these data makes for relatively straightforward analysis, indicating as it does an absence of complication from pre-indentation surface stresses and multi-region crack velocity functions. Accordingly, the solid curve in Fig. 2 is a theoretical fit of Equation 5 of [1], evaluated from the combined inert and fatigue strength data as follows:

(a) Taking the inert strength parameters $\sigma_m = 146 \pm 6$ MPa and $c_m = 98 \pm 15$ μm from Section 2.2, the composite equilibrium quantities K_c/χ_r and $K_c/(\pi\Omega)^{1/2}$ are evaluated as 83 ± 20 and 1.93 ± 0.20 MPa $m^{1/2}$ respectively from Equation 3 in [1].

(b) From a linear regression analysis of $\log \sigma$ against $\log \dot{\sigma}_a$ for the fatigue strength data represented in Fig. 2 (but using individual points rather than mean values) values of the slope, $1/(n' + 1) = 0.0112 \pm 0.0013$ and intercept, $(\log \lambda')/(n' + 1) = 2.055 \pm 0.003$ (expressed in terms of the units displayed on the axes in Fig. 2) are obtained as per Equation 2, from which the "apparent" kinetic parameters $n' = 89 \pm 10$ and $\log \lambda' = 184 \pm 20$ follow. Then Equation 14 of [1] is used in conjunction with the values of σ_m and c_m, to evaluate "true" kinetic parameters $n = 116 \pm 13$ and $\log (v_0/\text{m sec}^{-1}) = 5.0$. (All errors quoted in this paragraph are standard errors.)

(c) Now the dynamic fatigue curve is determined from Equation 5 of [1] by solving numerically to obtain the failure stress, σ, for specified values of stress rate $\dot{\sigma}_a$, with an indentation load at $P = 20$ N and an actual measured crack size c_0' of 69 μm as the initial condition.

The quality of fit between the curve thus generated and the data points may be taken as a measure of the validity of the indentation theory. In this context it should be noted that the procedure just outlined involves more than mere curve fitting: in regenerating the fatigue curve we are reliant on the accuracy of the transformation equations for converting kinetic parameters from apparent to true values (these equations themselves embodying several assumptions) and of the calibration of the inert strength parameters. Essentially, the exercise may be seen as a test of the residual-stress hypothesis for contact-induced flaws, in the sense that the key relations used in the parameter evaluations above (namely Equations 3 and 14 of [1]) contain the term χ_r (either explicitly or implicitly) as a vital element in the formulation.

Turning to Fig. 3, we may now attempt to explain the results for the machined surfaces in terms of simple departures from the idealized behaviour of the base-line curve for polished surfaces. Considering first the machined surfaces with indentations, we have already indicated (Section 2.2) that the elevation of strength above the base-line is attributable to the presence of a pre-intendation surface compressive stress layer. However, such a compressive stress cannot be acting uniformly over the entire indentation-crack area, for, if it were, according to Fig. 7 of [1], the fatigue plot would tend to a non-linear curve with reduced slope in the low stress-rate region; if anything, the curve for machined surfaces tends

to a greater slope than for polished surfaces at the left-hand side of the figure. In the high stress-rate region, on the other hand, the curve shows a distinctive upward rise toward the inert strength plateau reminiscent of the trends depicted in Fig. 6 of [1], for crack growth with Region II behaviour in the crack velocity response. As to the machined surfaces without indentations, we are constrained by the limited range of data to the observation that the results appear to be following the trends of the curve immediately below more closely than those of the base-line curve, suggesting that the machining flaws themselves respond in a manner similar to the indentation-induced radial cracks within the field of the compressive layer.

4. Discussion and conclusions

4.1. Assessment of the indentation-flaw method for fatigue analysis

The results obtained in the present study demonstrate the simplicity and economy of the indentation-flaw approach to fatigue analysis, particularly from the standpoint of material evaluation. In the context of this last point, it is useful to compare our kinetic parameter evaluations with those of Pletka and Wiederhorn [4] on the same batch of Pyroceram glass-ceramic. These authors studied the macroscopic crack-growth characteristics, using double-torsion test-pieces, as well as the fatigue-strength properties (Fig. 3). Their double-torsion data showed considerable shifts in the crack-velocity curves $v(K)$ from run to run, which was attributed to a systematic effect due to microstructural interactions with the crack as the fracture path lengthened. Notwithstanding this complication, Pletka and Wiederhorn obtained a mean estimate of $n = 83.5$ for the crack velocity exponent in Equation 4 of [1]. Our value of $n = 116$ is somewhat higher than theirs, but the difference is probably not significant in view of the experimental scatter in the two sets of data. A more graphic comparison of the results may be drawn from Fig. 4, in which we have plotted the crack velocity curve as reconstructed from Equation 4 of [1], using our own determinations of n and v_0, and $K_c = 2.5\ \text{MPa m}^{1/2}$ obtained by independent double-torsion and ("calibrated") indentation procedures [7, 8] along with the direct results of Pletka and Wiederhorn. (It is interesting to note that two other groups of workers, also using the double-torsion technique but on Pyroceram specimens from different billets, obtained $n = 55$ [9] and $n = 85$ [10], thus demonstrating the variability of results that can be obtained under what may appear at first sight to be the same conditions of testing.) Pletka and Wiederhorn also attempted to determine the crack velocity exponent from their dynamic fatigue data, but made no attempt to allow for residual-stress effects; their mean estimate, $n = 62.5$, must accordingly be regarded as systematically low, for the reasons touched on earlier in Section 3.

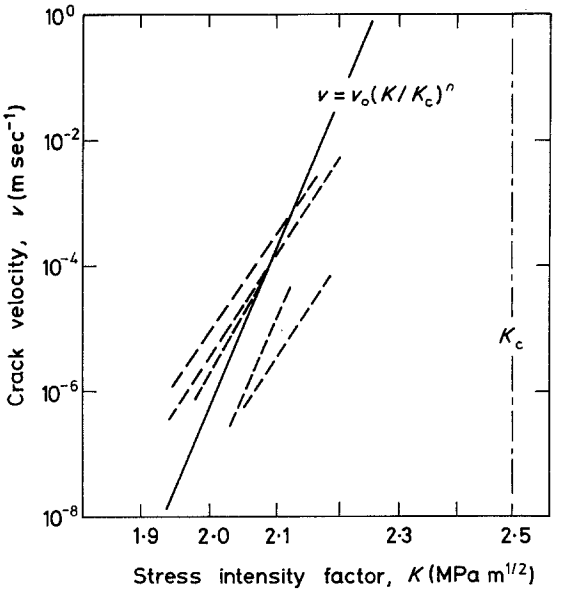

Figure 4 Crack velocity function of Pyroceram glass-ceramic in water. The solid line is a reconstruction of Equation 4 of [1], using fracture parameters determined from the analysis of Section 3. Dashed lines are results of several runs made by Pletka and Weiderhorn [4], using double-torsion test-pieces.

The apparent ability to reconstruct the macroscopic $v(K)$ function from fatigue data on as-indented surfaces needs to be taken cautiously. It will be recalled from Fig. 3 that the fatigue curve for machined surfaces with indentations shows evidence of Region II influence whereas the corresponding curve for polished surfaces does not. This difference in behaviour is consistent with the existence of a residual compression layer in the machined surfaces, as previously described. Under normal testing conditions (i.e. surfaces free of pre-existing stresses) the indentation flaw is most likely to fail from one of its points of intersection with the specimen free surface, where the residual-contact forces are strongest [11]. These points are, of course, always directly

exposed to the environment. Thus, with polished surfaces it is reasonable to expect that any transport-controlled Region II which shows up at higher velocities in data from macroscopic test-pieces with internal crack fronts, such as the double-torsion configuration, might be absent altogether. (Even with macroscopic test-pieces there is some evidence, from the way that the inner portions of the crack front lag increasingly behind those outer portions adjacent to the specimen surfaces as the velocity increases, in support of this hypothesis [12, 13].) With the machined surfaces, however, the compressive stresses would tend to close up the indentation cracks in the surface region, and thereby increase the probability of failure from some subsurface point on the crack front. It would then be necessary to transport the moisture along the crack interface to this subsurface point; hence the inflection in the fatigue curve. In semi-quantitative support of this argument, it may be recalled from Section 2.2 that the level of compression is such as to increase inert strengths by some 45%; and since the indentation flaws are initially only slightly more severe than the machining flaws themselves, and accordingly must experience this compression over a significant portion of their depth, the crack-closure effect will clearly be substantial. Of course, once the cracks extend in depth, as they will do under fatigue conditions, the crack closure will exert a decreasing influence on the stress to failure. The tendency for the data for machined surfaces to move closer to the base-line curve at the low stress-rate end in Fig. 3 may be seen as a manifestation of this behaviour.

As a corollory to the points just discussed, it could be argued that surface machining, although certainly deleterious in the sense that it introduces a high density of severe flaws, could actually be used as a means of strengthening ceramics in certain applications. Such would be the case, for instance, where component surfaces are subject to strength degradation from spurious impact events involving sharp particles [14]. Comparison of the results in Fig. 3 illustrates the point clearly; for a given contact load the machined surfaces are considerably more resistant to degradation than are the polished surfaces. However, the progressive diminution in this enhanced resistance at slower stress-rates suggests that the potential benefits are not likely to be so great in long-lifetime applications. The existence, or otherwise, of Region II crack velocity effects in the fatigue data also carries design implications, especially in proof-testing procedures where the strength of surviving components can be strongly influenced by the form of the $v(K)$ function at the high end of the stress-intensity-factor range [15]. It is thus highly important that one should be able to characterize the primary flaw fully before applying conventional fracture mechanics concepts to failure prediction.

It is also important to appreciate the role played by the inert-strength "calibration" in the fatigue curve analysis of Section 3. The accuracy of the evaluated equilibrium and kinetic parameters (from Equations 3 and 14 of [1]) for insertion into the differential equation for dynamic fatigue (Equation 5 of [1]), and thence of the regenerated fatigue curve itself, is determined to a large extent by the accuracy of the quantities σ_m and c_m. In particular, we may note that the kinetic parameter v_0, which controls the lateral positioning of the curve in the logarithmic $\sigma(\dot{\sigma}_a)$ plot, is extremely sensitive to the value of σ_m for typical values of n' (see Equation 14b, [1]). On the other hand, large errors in the v_0 term are not likely to show up strongly in the plot, bearing in mind that the stress-rate axis generally covers several orders of magnitude. Viewed in this light, the standard deviation of about 4% quoted here for σ_m would appear to be reasonably small. The corresponding standard deviation of about 15% quoted for c_m appears relatively large, but it is to be remembered that our reference configuration (σ_m, c_m) refers to a *maximum* in the $\sigma_a(c)$ function of Equation 2 of [1], where small variations in applied stress correspond to large variations in crack size. In addition, of course, the possibility exists of *systematic* error in the measurements. With regard to c_m, the question of crack visibility arises; there must always be some uncertainty as to the exact location of the crack tip, even under the most favourable viewing conditions (e.g. with gold-coated surfaces of near-limiting optical resolution), particularly in materials with complex microstructures. Such systematic errors may be less important in σ_m, as long as the strengths are similarly affected in fatigue as in inert environments. This last condition is not always respected, however; in glass [16] and silicon [17] it has been shown that interaction effects due to the presence of lateral cracks about the contact zone are strongly felt in the inert strengths [16, 17] (where the radial and

lateral dimensions are comparable) but not in the fatigue strengths [16] (where the radials grow at the expense of the laterals). Again, the ultimate test of the overall accuracy of the parameter determinations lies in our ability to regenerate the dynamic fatigue curve, using Equation 5 of [1], through the experimental data points.

The point made above in relation to the variability of interaction effects in the radial crack evolution warrants further comment, for it implies a lack of constancy in the configurational terms Ω and χ_r for different materials, and, indeed, for any one given material at different stages of the crack evolution. If it were not for this implication we might feel justified in attempting to predetermine these terms, either by theoretical analysis or by empirical calibration [1]. We would then be in a position to compute values of c_m *a priori* from Equation 3 of [1], thereby circumventing the need for any direct crack measurements on specially prepared test-pieces (as described in Section 2.2). Thus, for instance, if we were to take the crack-geometry parameter $\Omega = 4/\pi^2$ for an ideal, centrally-loaded penny crack [1], together with $\sigma_m = 146$ MPa and $K_c = 2.5$ MPa $m^{1/2}$ as qouted earlier for Pyroceram, we would obtain from Equation 3a the crack size $c_m = 130\,\mu m$; this compares with the value 98 μm from optical microscopy. A similar procedure could be followed using Equation 3b, allowing in this case that χ_r is a material-dependent quantity which depends on the ratio of elastic modulus to hardness [7, 11]. It is suggested here that until a complete understanding of all the factors which determine these configurational terms is available the most reliable route to the crack-scale parameter remains via direct measurement by conventional microcsopy.

4.2. Recomended test procedure

In concluding this study, we may re-emphasize some of the major advantages of using controlled flaws for fatigue analysis. The method is simple, requiring only the facility to make routine hardness indentations are conventional test-pieces. Whereas some care is needed in preparing the specimen surface, no further treatment is necessary once the indentations have been made; the existence of residual contact stresses is fully accommodated within the theoretical framework. The method is reasonably economical; less than 100 specimens have been used in compiling the Pyroceram data in Fig. 2. Reproducibility in results is relatively high, and the fracture parameters evaluated from the fatigue curves are representative (subject to the qualifications indicated in Section 4.1) of macroscopic crack velocity functions. In short, the indentation approach is well suited to the evaluation of materials properties for lifetime predictions, with special relevance to the micromechanics of naturally occurring flaws [1].

With these points in mind, our recommended procedure for the fatigue testing of ceramics using indentation flaws is as follows:

(a) Test-pieces for failure in flexure should be prepared in the usual way. The prospective tensile surfaces should be polished with 1000-grit SiC in water slurry until all built-in surface stresses due to machining or sawing damage are removed. Selected surfaces should be polished further with 1 μm diamond paste to an optically smooth finish for crack-size measurements.

(b) The samples should be indented with a Vickers diamond pyramid at the centre of the polished surface, the load being chosen so as to produce a well-defined crack pattern consistent with the scale of microstructure, specimen dimensions, etc. Additional dummy indentations may be added as required on the mirror-smooth surfaces. For tests in four-point bending, the indenter should be oriented such that one set of radial arms lies normal to the tensile direction. (With biaxial tests such orientation considerations are unnecessary.)

(c) Inert strength data should be obtained in dry argon or nitrogen (or in some other non-reactive environment) at the fastest practical stress rate. This determines σ_m. Crack dimensions at surviving indentations on the mirror-smooth surfaces should be measured, and c_m and c_0' thus obtained. (With biaxial tests *both* sets of orthogonal radial arms will give a measure of c_m, in which case an estimate of c_0' would need to be made from crack measurements prior to stressing to failure.) The condition $c_0' < c_m$ should then be confirmed. From these results the requisite equilibrium fracture parameters can be computed.

(d) Dynamic fatigue strengths should be measured over as wide a range of stress rates as practicable. The data should be fitted to the linear region of $\log \sigma$ against $\log \dot{\sigma}_a$, using least squares methods, to obtain n' and $\log \lambda'$. Then transformation relations should be used to determine "true" kinetic parameters n and v_0.

(e) If a check of the analysis is considered desirable, then the calibrated equilibrium and

kinetic fracture parameters should be taken and the dynamic fatigue curve regenerated from the basic differential equation of crack growth at the given indentation load, using the measured value of c_0' as the initial crack size. The degree of fit between the computed curve and the data points can be used as an indication of the accuracy of the analysis.

Acknowledgements

The authors express their gratitude to S. M. Widerhorn and B. J. Pletka for providing the Pyroceram glass-ceramic specimens, and for many discussions on the results. D. B. Marshall, T. P. Dabbs, P. Chantikul and P. L. Kelly made valuable contributions through their comments and assistance in the laboratory. Funding was provided by the Australian Research Grants Committee.

References

1. B. R. LAWN, D. B. MARSHALL, G. R. ANSTIS and T. P. DABBS, *J. Mater. Sci.* **16** (1981) 2846.
2. G. J. BANSAL, W. H. DUCKWORTH and D. E. NIESZ, *Amer. Ceram. Soc. Bull.* **55** (1976) 289.
3. B. J. PLETKA and S. M. WEIDERHORN, in "Fracture Mechanics of Ceramics", edited by R. C. Bradt, D. P. H. Hasselman and F. F. Lange (Plenum Press, New York, 1978), Vol. 4, p. 745.
4. B. J. PLETKA and S. M. WEIDERHORN, *J. Mater. Sci.* 17(5) (1982), to be published.
5. R. F. COOK, B. R. LAWN, T. P. DABBS and P. CHANTIKUL, *Commun. Amer. Ceram. Soc.*, **64** (1981) C-121.
6. D. B. MARSHALL, B. R. LAWN and P. CHANTIKUL, *J. Mater. Sci.* **14** (1979) 2225.
7. G. R. ANSTIS, P. CHANTIKUL, B. R. LAWN and D. B. MARSHALL, *J. Amer. Ceram. Soc.* **64** (1981) 533.
8. P. CHANTIKUL, G. R. ANSTIS, B. R. LAWN and D. B. MARSHALL, *J. Amer. Ceram. Soc.* **64** (1981) 539.
9. G. K. BANSAL and W. H. DUCKWORTH, *J. Mater. Sci.* **13** (1973) 239.
10. B. G. KOEPKE, unpublished work.
11. B. R. LAWN, A. G. EVANS and D. B. MARSHALL, *J. Amer. Ceram. Soc.* **63** (1980) 574.
12. K. SCHÖNERT, H. UMHAUER and W. KLEMM, "Fracture 1969", Proceedings of the Second International Conference on Fracture, Brighton, April 1969, edited by P. L. Pratt (Chapman and Hall, London, 1969), p. 474.
13. T. A. MICHALSKE, J. R. VARNER and V. D. FRECHETTE, in "Fracture Mechanics of Ceramics", edited by R. C. Bradt, D. P. H. Hasselman and F. F. Lange (Plenum Press, New York, 1978), Vol. 4, p. 639.
14. B. R. LAWN and D. B. MARSHALL, in "Fracture Mechanics of Ceramics", edited by R. C. Bradt, D. P. H. Hasselman and F. F. Lange (Plenum Press, New York, 1978), Vol. 3, p. 205.
15. E. R. FULLER, S. M. WEIDERHORN, J. E. RITTER, and P. B. OATES, *J. Mater. Sci.* **15** (1980) 2282.
16. D. B. MARSHALL and B. R. LAWN, *J. Amer. Ceram. Soc.* **63** (1980) 532.
17. B. R. LAWN, D. B. MARSHALL and P. CHANTIKUL, *J. Mater. Sci.* **17** (1981) 1769.

Received 27 July
and accepted 15 September 1981